Acta Cryst C STRUCTURAL CHEMISTRY

ISSN 2053-2296

Crystal structures, electron spin resonance, and thermogravimetric analysis of three mixed-valence copper cyanide polymers

Peter W. R. Corfield,* Ahmed Elsayed, Tristan DaCunha and Christopher Bender

Department of Chemistry and Biochemistry, Fordham University, 441 East Fordham Road, Bronx, NY 10458, USA. *Correspondence e-mail: pcorfield@fordham.edu

Received 23 March 2024
Accepted 16 April 2024

Edited by R. Diniz, Universidade Federal de Minas Gerais, Brazil

Keywords: crystal structure; mixed valence; copper cyanide; ethanolamine; propanolamine; polymeric network; electron spin resonance; ESR; thermogravimetric analysis; TGA.

CCDC references: 2348772; 2348771; 2348770

Supporting information: this article has supporting information at journals.iucr.org/c

The crystal structures of three mixed-valence copper cyanide alkanolamine polymers are presented, together with thermogravimetric analysis (TGA) and electron spin resonance (ESR) data. In all three structures, a Cu^{II} moiety on a crystallographic center of symmetry is coordinated by two alkanolamines and links two $Cu^{I}CN$ chains *via* cyanide bridging groups to form diperiodic sheets. The sheets are linked together by cuprophilic Cu^{I}–Cu^{I} interactions to form a three-dimensional network. In poly[bis(μ-3-aminopropanolato)tetra-μ-cyanido-dicopper(I)dicopper(II)], $[Cu_4(CN)_4(C_3H_8NO)_2]_n$, **1**, propanolamine bases have lost their hydroxyl H atoms and coordinate as chelates to two Cu^{II} atoms to form a dimeric Cu^{II} moiety bridged by the O atoms of the bases with Cu^{II} atoms in square-planar coordination. The ESR spectrum is very broad, indicating exchange between the two Cu^{II} centers. In poly[bis(2-aminopropanol)tetra-μ-cyanido-dicopper(I)copper(II)], $[Cu_3(CN)_4(C_3H_9NO)_2]_n$, **2**, and poly[bis(2-aminoethanol)tetra-μ-cyanido-dicopper(I)copper(II)], $[Cu_3(CN)_4(CH_7NO)_2]_n$, **3**, a single Cu^{II} atom links the $Cu^{I}CN$ chains together *via* CN bridges. The chelating alkanolamines are not ionized, and the OH groups form rather long bonds in the axial positions of the octahedrally coordinated Cu^{II} atoms. The coordination geometries of Cu^{II} in **2** and **3** are almost identical, except that the Cu—O distances are longer in **2** than in **3**, which may explain their somewhat different ESR spectra. Thermal decomposition in **2** and **3**, but not in **1**, begins with the loss of HCN(g), and this can be correlated with the presence of OH protons on the ligands in **2** and **3**, which are not present in **1**.

1. Chemical context

Polymeric CuCN compounds with organic ligands have continued to excite interest in light of their varied structures (Pike, 2012), the magnetic exchange or photoluminesence exhibited by many of them, and other potentially useful physical properties (Lim *et al.*, 2008). Many hundreds of crystal structures are now known (*e.g.* Nicholas *et al.*, 2019; Xu *et al.*, 2019; Etaiw *et al.*, 2016). One class of such polymers comprises anionic CuCN frameworks with guest cations providing charge neutrality and we have made systematic studies of such compounds containing cations derived from amines and ethanolamines (Koenigsmann *et al.*, 2020; Corfield *et al.*, 2022). Mixed-valence CuCN polymers containing bases coordinated to the Cu^{II} atoms are also well known (Liu *et al.*, 2017; Qin *et al.*, 2016), though fewer in number than the $Cu^{I}CN$ complexes. Such networks would be neutral not anionic, and might therefore be capable of crystallizing with neutral molecules as guests. We have made studies of several such complexes involving diamines (Corfield *et al.*, 2016), but until recently we were less successful at isolating crystalline complexes of mixed-valence CuCN networks involving

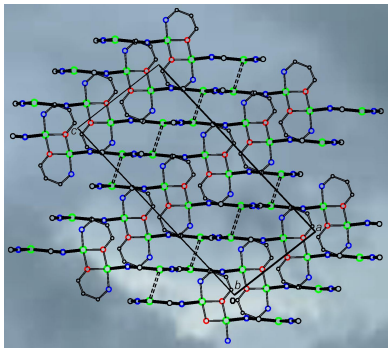

N-substituted ethanolamines. In the present article, we describe the isolation and structural characterization of crystals of three such mixed-valence CuCN networks, along with powder ESR data and thermogravimetric analyses: poly[bis(μ-3-aminopropanolato)tetra-μ-cyanido-dicopper(I)dicopper(II)], **1** (Scheme 1), with the base propanolamine, coordinated to Cu^{II} as an alkoxide; poly[bis(2-aminopropanol)tetra-μ-cyanido-dicopper(I)copper(II)], **2** (Scheme 2), with the base 2-aminopropan-1-ol; and poly[bis(2-aminoethanol)tetra-μ-cyanido-dicopper(I)copper(II)], **3** (Scheme 3), with the base ethanolamine.

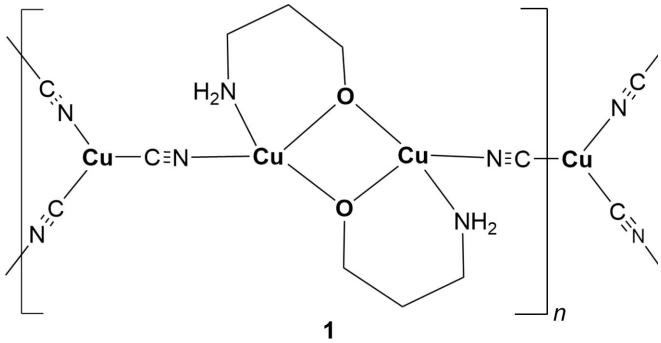

1
Scheme 1

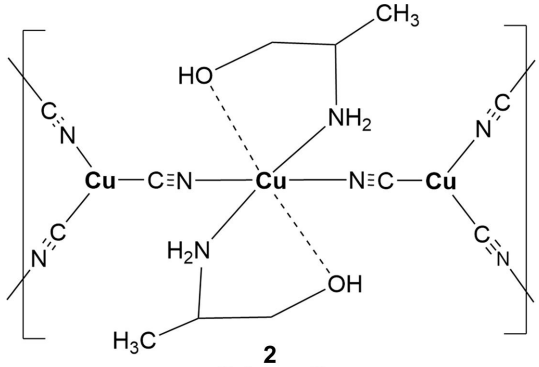

2
Scheme 2

2. Experimental

2.1. Synthesis and crystallization

Syntheses were carried out by air oxidation of solutions containing NaCN/CuCN in the presence of the amine ligand. Results varied from batch to batch. Specific details of representative syntheses follow.

For the preparation of **1**, 17 mmol (0.833 g) of NaCN were dissolved in 25 ml of distilled water and 15 mmol (1.343 g) of CuCN were added and the mixture stirred and filtered, as not quite all of the CuCN had dissolved. Then 35 mmol of 3-aminopropan-1-ol (2.629 g) were added with stirring, and the colorless mixture was covered. Red crystals separated after about two weeks (yield: 0.393 g, or 21%, based upon Cu). IR spectra (cm^{-1}): 2124 (*s*), 2135 (*s*) (CN stretch); 3255 (*s*), 3298 (*s*) (N—H stretch); 3452 (*m*) (O—H stretch, broad, probably due to moisture contaminant). Preparations under similar conditions did not always produce homogeneous samples, but crystals of **1** were usually present.

For the preparation of **2**, 20 mmol (0.995 g) of NaCN were dissolved in 20 ml of distilled water and 10 mmol (0.893 g) of CuCN were added. The mixture was stirred until a clear solution was obtained. 20 mmol (1.502 g) of 2-aminopropan-1-ol were added and the mixture stirred. After about three months, 38 mg of a brown product composed of gold–brown plates were obtained. Based upon a molecular formula of $Cu_3(CN)_4L_2$, where L = 2-aminopropan-1-ol, this corresponds to a percentage yield of 2.6%. IR spectra (cm^{-1}): 2104 (*s*), 2116 (*s*) (CN stretch); 3255 (*m*), 3319 (*m*), 3347 (*w*) (N—H stretch); 3506 (*m*), 3543 (*m*) (O—H stretch). We were surprised to also obtain 184 mg of a crystalline material that gave the same IR spectrum in a separate synthesis designed to give a $Cu^{I}CN$ complex only. In this case, we used the same procedure, with 5.0 mmol of CuCN instead of 10 mmol, but the base was neutralized before addition to the aqueous NaCN/CuCN mixture, which we presumed would hinder air oxidation of Cu^{I}. We do not have an explanation for this synthesis when so many other attempts had been unsuccessful.

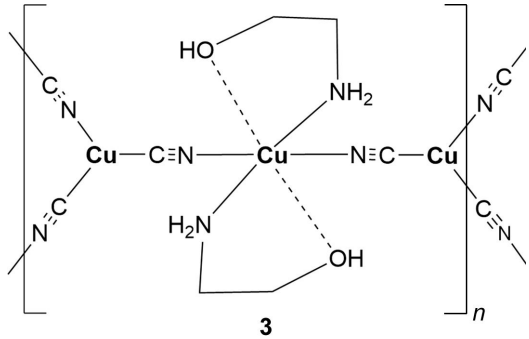

3
Scheme 3

For the preparation of **3**, 39 mmol (1.898 g) of NaCN were dissolved in 8 ml of distilled water and 23 mmol (2.080 g) of CuCN were added, and the mixture stirred until a clear solution was obtained. 21 mmol (1.293 g) of 2-aminoethanol in 3 ml water were added, and the pale-green mixture stirred. After 5 d, 223 mg of black crystals were obtained, corresponding to a 6.9% yield based on Cu. IR spectra (cm^{-1}): 2118 (*s*), 2130 (*s*) (CN stretch); 3266 (*m*), 3233 (*m*) (N—H stretch); 3524 (*m*) (O—H stretch).

2.2. Refinement

Crystal data, data collection and structure refinement details are summarized in Table 1. For structures **2** and **3**, the tensor analysis in *XABS2* (Parkin *et al.*, 1995) was used to improve the absorption correction, leading to a somewhat less noisy final difference Fourier map. In all structures, C—H protons were restrained to the expected geometry, with C—H distances of 0.97 Å, while positional coordinates for N—H and O—H protons were refined. For C—H hydrogens, the U_{iso}(H) values were constrained to $1.2U_{eq}$ of the adjacent atoms for **1**, and $1.5U_{eq}$ for **2** and **3**. In **1**, the low-angle 020 reflection was omitted as it was partially obscured by the beamstop. For **3**,

Table 1
Experimental details.

Experiments were carried out at 295 K with Mo $K\alpha$ radiation using an Enraf–Nonius KappaCCD diffractometer. The absorption correction was part of the refinement model (ΔF) (Otwinowski & Minor, 1997). H atoms were treated by a mixture of independent and constrained refinement.

	(1)	(2)	(3)
Crystal data			
Chemical formula	$[Cu_4(CN)_4(C_3H_8NO)_2]$	$[Cu_3(CN)_4(C_3H_9NO)_2]$	$[Cu_3(CN)_4(C_2H_7NO)_2]$
M_r	506.48	444.94	416.88
Crystal system, space group	Monoclinic, $C2/c$	Monoclinic, $P2_1/c$	Monoclinic, $P2_1/c$
a, b, c (Å)	9.6829 (4), 8.2557 (4), 21.4992 (10)	9.3903 (4), 8.9608 (4), 9.7986 (4)	9.5158 (2), 8.8022 (2), 9.3589 (2)
β (°)	95.212 (3)	112.134 (3)	117.358 (1)
V (Å^3)	1711.52 (14)	763.74 (6)	696.22 (3)
Z	4	2	2
μ (mm^{-1})	4.91	4.15	4.55
Crystal size (mm)	0.31 × 0.15 × 0.08	0.15 × 0.08 × 0.02	0.37 × 0.25 × 0.22
Data collection			
T_{min}, T_{max}	0.364, 0.514	0.75, 0.93	0.48, 0.59
No. of measured, independent and observed [$I > 2\sigma(I)$] reflections	19341, 1965, 1501	19192, 1350, 855	27010, 1740, 1049
R_{int}	0.048	0.084	0.046
$(\sin\theta/\lambda)_{max}$ (Å^{-1})	0.649	0.595	0.678
Refinement			
$R[F^2 > 2\sigma(F^2)]$, $wR(F^2)$, S	0.025, 0.074, 1.09	0.034, 0.113, 1.16	0.024, 0.077, 1.16
No. of reflections	1965	1350	1740
No. of parameters	124	117	118
No. of restraints	0	28	26
$\Delta\rho_{max}$, $\Delta\rho_{min}$ (e Å^{-3})	0.46, −0.42	0.84, −0.48	1.07, −0.53

Computer programs: *KappaCCD Server Software* (Nonius, 1997), *SCALEPACK* (Otwinowski & Minor, 1997), *DENZO* (Otwinowski & Minor,1997), *SHELXT* (Sheldrick, 2015*a*), *SHELXS97* (Sheldrick, 2008), *SHELXL2018* (Sheldrick, 2015*b*), *ORTEPIII* (Burnett & Johnson, 1996), *ORTEP-3 for Windows* (Farrugia, 2012) and *publCIF* (Westrip, 2010).

data sets from two crystals were merged using *SORTAV* (Blessing, 1989). The size of the second smaller crystal was 0.15 × 0.10 × 0.06 mm.

In all three structures, CN group occupancies were refined, initially set with 50% disorder. The occupancies for all CN groups bound to Cu^{II} clearly indicated that these groups are *N*-bonded to Cu^{II}, as expected, while the refined occupancies for the CN groups linking Cu^{I} atoms were not significantly different from 50%. Thus, only the Cu^{I} CN groups were modeled as disordered and were fixed at 50% in all structures.

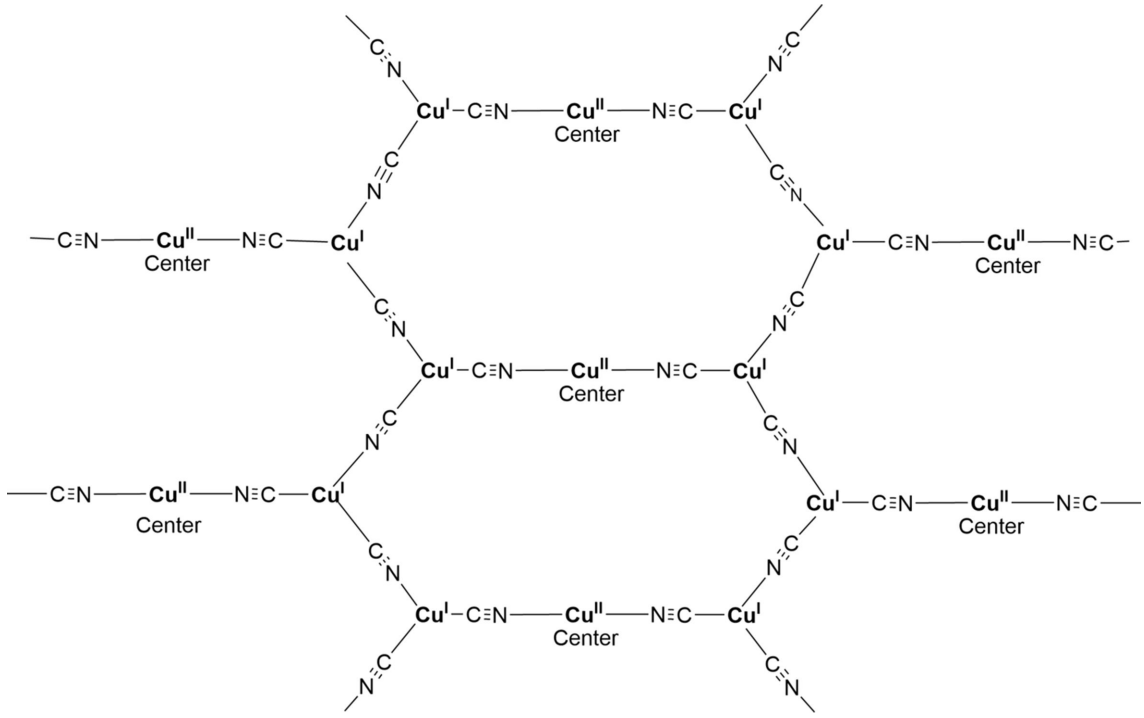

Figure 1
General scheme for the title compounds.

Table 2
Comparison of selected bond lengths (Å) and angles (°) for **1**, **2** and **3**.

	1	**2**	**3**
	1.901 (2), 1.923 (2)	2.56 (13), 2.64 (11)	2.439 (14), 2.67 (3)
Cu2—NH_2	1.976 (3)	2.054 (5)	2.044 (3)
Cu2—NC	1.922 (2)	1.969 (5)	1.963 (2)
C2—Cu1—N2, *trans* to Cu1—C1/N1—Cu2	111.63 (10)	121.7 (2)	120.78 (11)

In **1**, atoms C12, C13, and C14 of the chelate ring Cu2/O11/C12–C14/N15/Cu2 were treated as disordered above and below the central plane of the six-membered ring, and the *A*/*B* occupancies refined to 74 (2) and 26 (2)%. In both **2** and **3**, the chelating ethanolamine ligands were modeled as disordered between λ and δ conformations. All the ligand atoms were counted as disordered, except that the tightly bound NH_2 atoms of the two disorder mates were constrained in both structures to the same positions, whereas the more loosely bound OH atoms were allowed to refine independently, along with the ligand C atoms, with constraints on the displacement parameters for the O atoms. The *A*/*B* occupancies refined to 53.4 (9) and 46.6 (9)% for **2**, and to 64.3 (16) and 35.7 (16)% for **3**.

3. Results and discussion

3.1. Structural commentary

In each of the three title structures, a Cu^{II} moiety coordinated by chelated alkanolamine bases links zigzag $Cu^{I}CN$ chains into a diperiodic network *via* bridging CN groups, with the Cu^{II} moiety situated at a crystallographic center of symmetry, as seen in the general scheme (Fig. 1). In every case, the C atoms of the chelated rings are disordered. For convenience, we have labeled Cu^{I} atoms as Cu1 and Cu^{II} atoms as Cu2 in the discussion that follows.

In the structure of **1**, shown in Fig. 2, the propanolamine bases have lost their hydroxyl H atoms, and coordinate as chelates to two Cu2 atoms to form a dimeric Cu^{II} moiety bridged by the O atoms of the bases to form a central four-atom ring. The eight central Cu, N, and O atoms of the dimeric moiety are roughly coplanar, with r.m.s. deviation from the best plane of 0.023 Å. The Cu2 atoms are in a distorted square-planar coordination, with the O—Cu—O angle in the four-membered ring equal to 76.91 (8)° and the other bond angles ranging from 91.15 (11) to 96.64 (9)°. The fourth ligand to each Cu2 atom is a CN group which bridges to a Cu1 atom bonded to two other CN groups. The bond angles at Cu1 are 111.63 (10), 122.02 (10), and 125.89 (10)°, with the smallest angle *trans* to the CN bridging to Cu2.

Figs. 3 and 4 show the asymmetric units for structures **2** and **3**, where single Cu2 atoms play the role of the dimeric moieties in **1** in linking the Cu1 chains into diperiodic structures. Cu2 atoms are octahedrally coordinated by two cyanide groups and by two chelating ligands, which are disordered between λ and δ conformations. The coordination is illustrated in Fig. 5, and comparisons of bond lengths and angles with **1** are given in Table 2. The coordination geometries are almost identical for compounds **2** and **3**. In these two structures, the ligands have not lost their OH protons and the Cu—O distances are much longer than in **1** where the bonding is to an alkoxide. The Cu—NH_2 and Cu—NC bonds are also slightly longer in **2** and

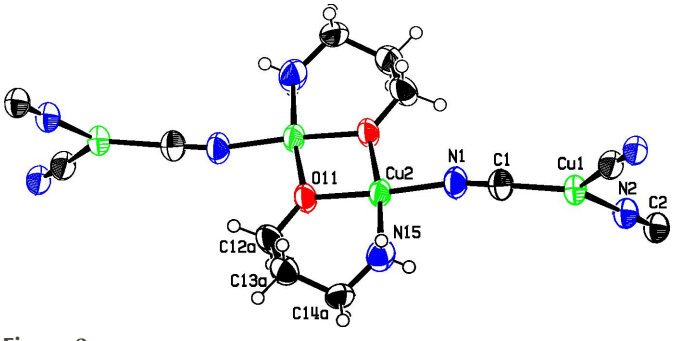

Figure 2
The structure of **1**, showing the atom numbering and 50% displacement ellipsoids, with H atoms depicted as small spheres. Only the major-disorder component for the chelate ring is shown. Cu atoms are shown in green, N atoms in blue, O atoms in red, and C and H atoms in black. The asymmetric unit is highlighted in bold.

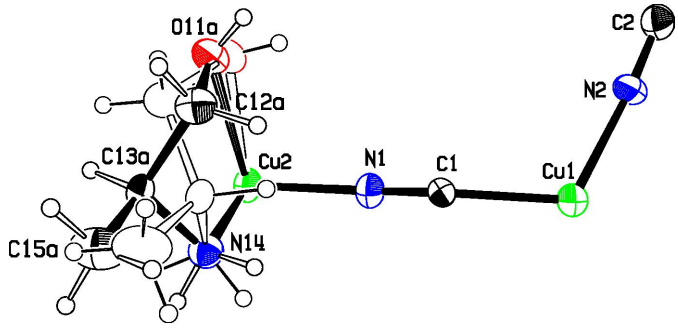

Figure 3
The asymmetric unit of **2**, showing the atom numbering and 50% displacement ellipsoids. The colors are as in Fig. 2.

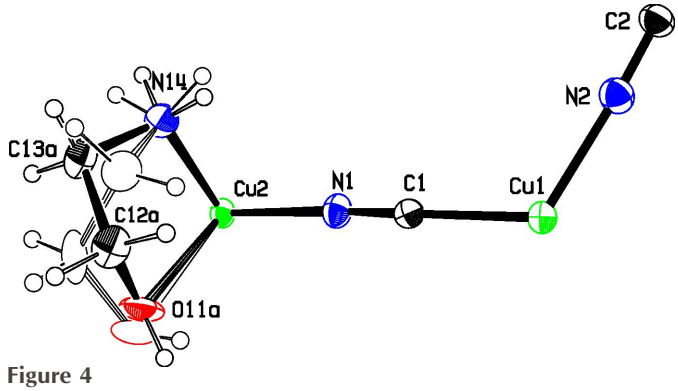

Figure 4
The asymmetric unit of **3**, showing the atom numbering and 50% displacement ellipsoids. The colors are as in Fig. 2.

Table 3
Hydrogen-bond geometry (Å, °) for **2**.

D—H···A	D—H	H···A	D···A	D—H···A
N14A—H14A···O11A^{i}	0.89	2.48	3.21 (11)	140
O11B—H11B···N2^{ii}	0.82 (2)	2.54 (13)	3.28 (11)	150 (13)
C12A—H12A···C2N^{ii}	0.97	2.54	3.29 (2)	134

Symmetry codes: (i) $-x, y-\frac{1}{2}, -z+\frac{1}{2}$; (ii) $x, -y+\frac{1}{2}, z+\frac{1}{2}$.

Table 4
Hydrogen-bond geometry (Å, °) for **3**.

D—H···A	D—H	H···A	D···A	D—H···A
N14B—H14D···O11B^{i}	0.89	2.20	3.09 (3)	178
O11B—H11B···N2C^{ii}	0.82 (1)	2.53 (6)	3.30 (3)	156 (11)

Symmetry codes: (i) $-x, y+\frac{1}{2}, -z+\frac{1}{2}$; (ii) $-x+1, -y, -z$.

3 than in **1**. The bond angles at Cu1 in **2** range from 113.4 (2) to 121.8 (2)°, while in **3** they range from 118.33 (12) to 120.78 (11)°. In both cases, the largest angle is *trans* to the CN bridging to Cu^{II}, in contrast to **1**, where there is a larger deviation of angles from 120° and the smallest angle is *trans* to the CN—Cu2 bridge.

The structure of **3** has been reported previously (Jin *et al.*, 2006), but was redone in our laboratory for consistency. In Jin *et al.*, the space group was given as *C*2/*m*. We chose *C*2/*c*, as in all crystals that we have studied, reflections with $k + l$ odd are present, though systematically weak; in *C*2/*m*, $k + l$ reflections would be absent, leading to a slightly different structure. Jin *et al.* did not record the presence of the OH proton, so that database searches based upon ethanolamine do not lead to their structure.

3.2. Supramolecular features

In **1**, the dimeric Cu2 moieties bridge monoperiodic Cu^{I}CN chains to form diperiodic networks parallel to (102), as shown in Figs. 6 and 7. The Cu^{I}CN zigzag chains extend in the direction of the *b* axis, out of the plane of Fig. 7. The plane of the Cu^{I}CN chain network makes an angle of 85.5 (1)° with the eight-atom dimeric Cu2 plane. Cu1 atoms from neighboring sheets are within 3.103 (1) Å of one another, in roughly axial positions with regard to their trigonal planar coordination. Also, the Cu1 atom lies 0.075 (2) Å out of the plane of its three ligands, which brings it closer to the neighboring Cu1 atom in the neighboring sheet. This weak cuprophilic interaction links the sheets into a triperiodic network, and is shown as a dashed line in Fig. 7. Atom H14*B* is found on the other side of the Cu1 coordination plane, at 3.10 Å from Cu1. Otherwise, there are no other short intermolecular contacts of note in this structure.

The structures of **2** and **3** have the same space group and very similar unit-cell dimensions. In both structures, the Cu2 moieties bridge monoperiodic Cu^{I}CN chains to form diperiodic networks parallel to (102), as shown in Figs. 8 and 9 for **2**, and in Figs. 10 and 11 for **3**. Inversion-related Cu1 atoms from neighboring sheets are 2.7400 (15) Å apart in **2** and 2.7734 (7) Å apart in **3**. In each structure, Cu1 atoms are

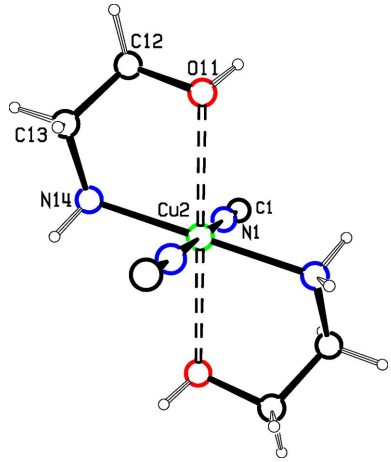

Figure 5
The Cu^{II} coordination in **3**. The coordination in **2** is the same, with a methyl group added to position C12.

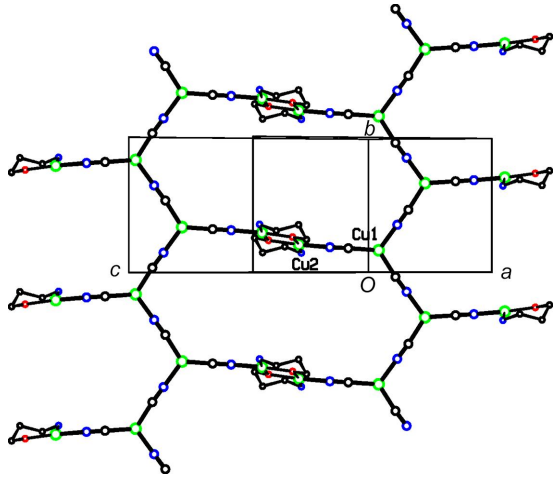

Figure 6
A diperiodic sheet in **1**. The colors are as in Fig. 2.

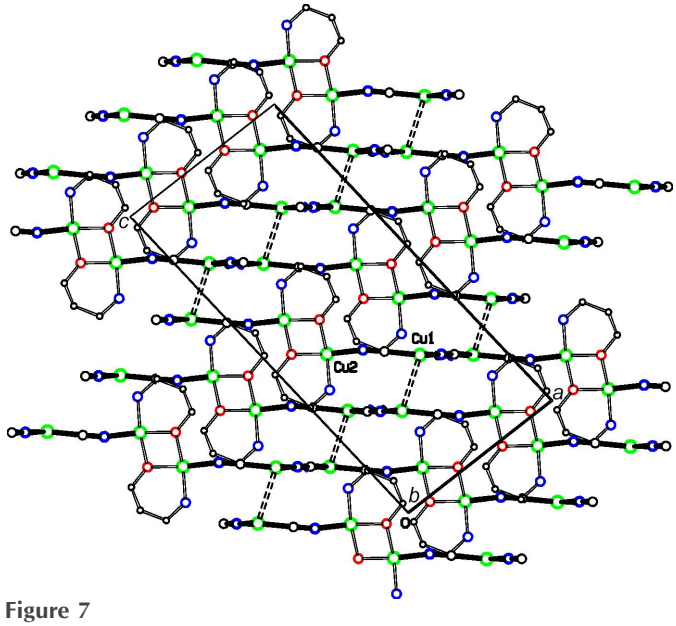

Figure 7
The packing in **1**. The sheets shown in Fig. 6 are viewed edge on. Putative cuprophilic bonds are shown as dashed double lines.

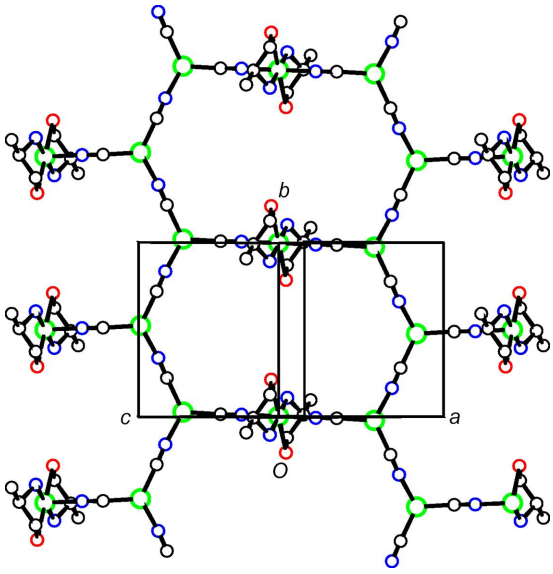

Figure 8
A diperiodic sheet in **2**. The colors are as in Fig. 2.

pulled out of the plane of their three coordinated atoms towards the neighboring inversion-related Cu1 atom, 0.302 (4) Å in **2** and 0.1774 (16) Å in **3**. In **2**, the C2 atom of cyanide C2N2 is also positioned somewhat close to the Cu1 atom of the neighboring sheet, at 2.502 (6) Å, which may indicate that the CN group could be regarded as μ_3-bonded, with very different Cu—C/N distances, rather than the μ_2-bonding that we have assumed. A similar situation exists for **3**, although here the Cu—C/N distance to the neighboring sheet is even longer, at 2.686 (3) Å.

Putative hydrogen bonds based on $D\cdots A \leq 3.30$ Å and D—H$\cdots A > 130°$ are listed in Tables 3 and 4 for compounds **2** and **3**, respectively. No contacts in **1** fit these criteria. For both compounds **2** and **3**, the NH_2 group is donor to a screw-related O atom, and one OH disorder component is donor to a C≡N group.

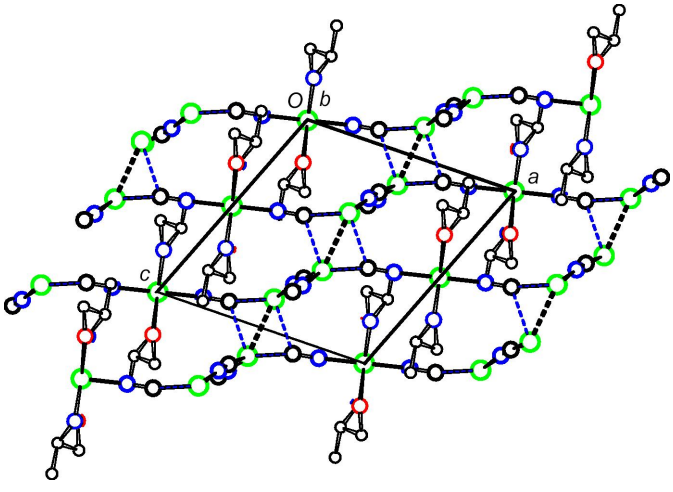

Figure 9
Packing in **2**. The sheets shown in Fig. 8 are viewed edge on. Putative cuprophilic bonds are shown as dashed double lines and putative μ_3-C—Cu bonds as blue single-dashed lines.

3.3. Electron spin resonance (ESR)

ESR spectra of the powdered sample materials were recorded at room temperature using a Bruker EMXnano operating at 9.63 GHz (X-band). For all samples reported here, spectral line shape was unaffected by incident microwave power (*i.e.* no saturable component of the inhomogeneously broadened line), and the general operating parameters were 0.3 mW (incident power); 2 Gauss (field modulation). Spectra were recorded without using the spectrometer's digital filter in 0.5 Gauss steps for a 1000 Gauss field sweep; the receiver signal acquisition time per step corresponded to four time constants.

The structure of **1** features two Cu^{II} ion centers bridged by oxygen, and the resultant ESR spectrum is a broad asymmetric singlet with a crossing point at $g = 2.24$ [Fig. 12(*a*)]. The absence of discernable *g*-anisotropy in the line shape is indicative of spin exchange, as is expected for a bridged binuclear center. The shape and *g*-value determined for this isotropic line is nearly identical to that obtained when a crystal of calcium copper acetate, which ordinarily has a well-defined anisotropic spectrum, is decomposed at 750 °C; the resulting ESR spectrum of this mixed metal oxide is a broad singlet with $g = 2.22$ (Bender, unpublished).

In contrast to the structure of **1**, the Cu^{II} centers of both structures **2** and **3** are mononuclear, and the corresponding polycrystalline ESR spectra possess line shape features that are rhombic in character (*cf.* Hathaway, 1971). The turning points in the spectrum of **2** [Fig. 12(*b*)], corresponding approximately to the diagonal components of the *g*-tensor, are $g_1 = 2.06$, $g_2 = 2.09$, and $g_3 = 2.20$. The three unequal pairs of coordinate bonds [*i.e.* bond lengths: 2.60 (Cu—O), 2.056 (Cu—N), and 1.967 Å (Cu—NC)], lead us to expect an elongated-rhombic octahedral configuration, and our data compare favorably with the literature values (*cf.* Hathaway, 1971).

The ESR spectrum of polycrystalline **3** [Fig. 12(*c*)] differs from that of structure **2**, presumably due to the reduced

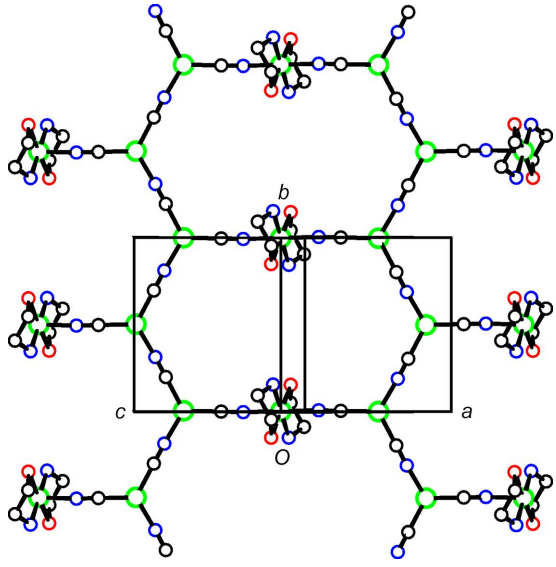

Figure 10
A diperiodic sheet in **3**. The colors are as in Fig. 2.

Table 5
Thermogravimetric analysis data.

Compound	**1**	**2**	**3**
Molecular formula	$Cu_4(CN)_4L'_2$	$Cu_3(CN)_4L''_2$	$Cu_3(CN)_4L'''_2$
L', L'', L'''	$NH_2(CH_2)_3O^-$	$NH_2CH(CH_3)CH_2OH$	$NH_2CH_2CH_2OH$
Molar mass, u	506.44	444.98	416.87
% Mass remaining at 400 °C	68.8	57.4	64.6
For Residue at 400 °C	Cu, C, H, N	Cu, C, H, N	Cu, C, H, N
Observed Cu, C, H, N %	73.0, 16.0, 0.17, 11.3	75.2, 14.6, 0.24, 9.8	70.8, 15.9, 0.13, 12.6
Calculated Cu, C, H, N %	72.8, 15.7, 0.00, 11.5	76.0, 14.4, 0.00, 9.6	71.3, 16.2, 0.00, 12.6
Assumed composition for % calculation	5CuCN + 2Cu + 3C	4CuCN + 3Cu + 3C	4CuCN + Cu + 2C

Cu—O distance. The shape of the line is rhombic in character, but lacks the added feature [labeled in Fig. 12(*b*) as 'g_3'] that is associated with elongation or its counterpart, compression (Hathaway, 1971). The *g*-values determined from the two turning points are $g' = 2.06$ and $g'' = 2.16$; the crossing point occurs at $g''' = 2.10$.

3.4. Thermogravimetric analysis (TGA)

TGA was carried out with a TA Instruments Q500 device. Samples of each compound weighing 5–20 mg were heated under nitrogen gas at 3° min^{-1} to 600 °C or more. The TGA plots up to 500 °C for the three compounds are shown in Fig. 13. (For **1**, analyses were complicated, as most samples were heterogeneous. The plot shown is for crystals hand-sorted under the microscope.) In all three compounds, there is a sharp drop in mass of 10–15% at 150–200 °C, followed by slower rates of mass loss. The absence of clear steps in the decomposition curves indicates overlapping of incremental decomposition changes. Not shown in the figure are the continued slow mass losses after 500 °C and the occasional subsequent mass increase, presumably due to the formation of an oxide of copper by reaction with residual oxygen in the system. Microscopic examination of residues obtained at the higher temperatures appeared to show mixtures of a black substance and metallic copper.

The decomposition curves for **2** and **3** differ more from each other than might have been expected from the similarity of the structures. In particular, there is a clear change in slope after a mass loss of about 8% for **2**, while the corresponding change is more gradual for **3**, and also the mass differences in the 350–400 °C range are more than would be anticipated based upon their molecular formulae.

From previous experiments in our laboratory, we expect any CuCN(s) formed to decompose to Cu(s) in the temperature range 400–500 °C. For this reason, each experiment was repeated with termination at 400 °C, in every case leaving black powdery residues. We obtained IR spectra and elemental analyses for each residue at this point, and the results are given in Table 5. All of the 400 °C residues showed IR peaks indicating the presence of CuCN(s) and, in all cases, the residues were richer in both Cu and C than expected for pure CuCN(s), while showing negligible presence of H. Total percentages ranged from 99.3 to 100.4%, precluding the presence of any significant amount of O. We have interpreted the residue composition in terms of mixtures of CuCN(s), C(s), and Cu(s), since it is assumed that any copper(I) acetylide formed would have decomposed by this tempera-

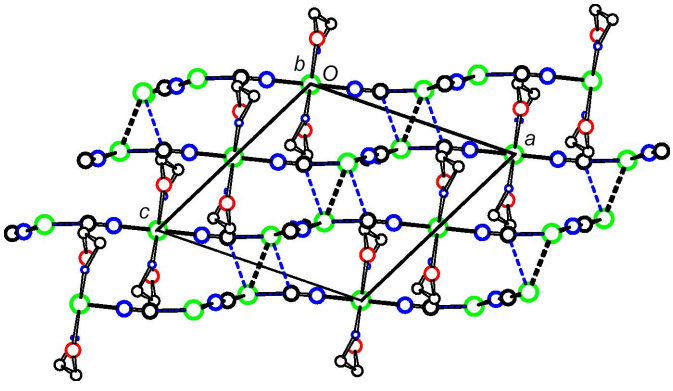

Figure 11
The packing in **3**. The sheets shown in Fig. 10 are viewed edge on. Putative cuprophilic bonds are shown as dashed double lines and putative μ_3-C—Cu bonds as blue single-dashed lines.

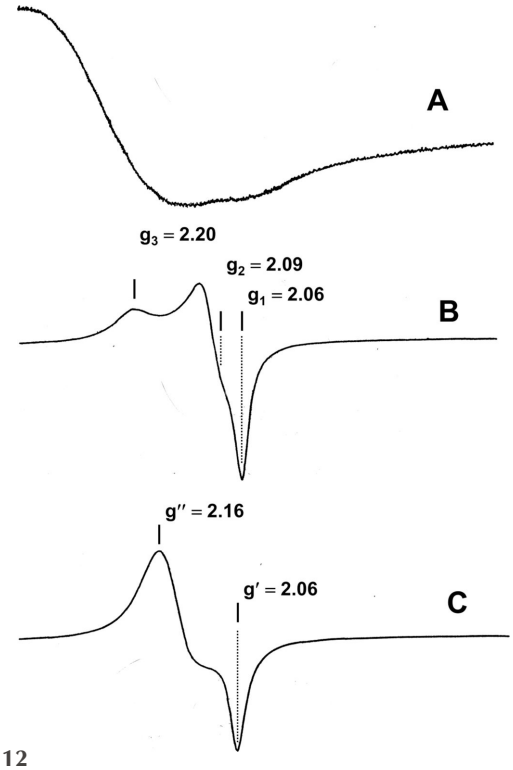

Figure 12
Electron spin resonance (ESR) spectra.

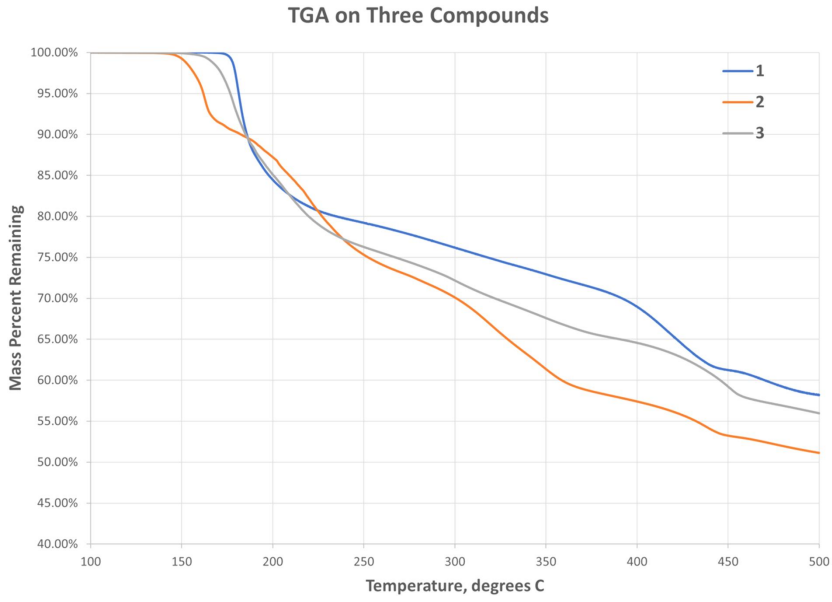

Figure 13
The thermal analysis results for the three compounds. The mass percentage remaining is plotted as a function of temperature.

ture, and the percentages calculated from the assumed mixtures are also given in Table 5. The observed %Cu values were calculated by dividing the %Cu expected from the molecular formula by the fraction of mass remaining at 400 °C. This, of course, assumes that the starting material was pure.

To check for HCN(g) emission at the initial stage, we heated 15–20 mg samples of each of the compounds in turn in a test tube, and looked for cloudiness in a drop of $AgNO_3$(aq) held over the mouth of the tube. Cloudiness in the $AgNO_3$ drop was clearly seen at sand-bath temperatures of 190–200 °C for **2** and 205–215 °C for **3**, but no evidence for HCN(g) emission was noted for **1**, even when the sample was held at or above 250 °C for several minutes.

It is possible that the CN groups bridging Cu1 and Cu2 in **2** and **3** are lost first, combining with the OH protons from the ligands coordinated to Cu2 to form HCN(g), which is not possible in **1**. This would leave the $Cu^{I}CN$ chains intact, while the deprotonated ligands would bind to Cu2 more tightly, as they do in **1**. Thereafter, for all three compounds, the bound ligands apparently lose their O and N moieties, while leaving at least some of the carbon present in elemental form. Apparently, this begins to happen in **1** before any cyanide loss.

3.5. Database survey

The neutral diperiodic mixed-valence CuCN network of the three structures described here has not often been noted. A search in the Cambridge Structural Database (CSD, Version 5.35; Groom *et al.*, 2016) found two similar structures (Kim *et al.*, 2005; Trivedi *et al.*, 2014). The first involves a CuCN network with Cu^{II} atoms coordinated by cyclam units and the second a more complex cyanide/azide network with Cu^{II} coordinated by NH_3.

A search for Cu compounds containing propanolamine, with or without the OH proton, yielded 48 hits. None of these structures involved Cu bonded to cyanide, however. Of these structures, 44 involved Cu_2O_2 units with chelating propanolate chelates, as found in **1**. Only seven of the structures contained the propanolamine ligand with the OH group intact bonded to Cu, with three of these also containing the Cu_2O_2 unit. A separate, more general, search of the CSD for dimeric Cu_2O_2 moieties with Cu bonded to two O and two N atoms yielded 258 hits, so that the four-membered ring of Cu_2O_2 is not uncommon.

A search for Cu coordinated by 2-aminopropan-1-ol gave seven hits. In all but one case (CSD refcode BOYPIO; Nieuwpoort *et al.*, 1983; Marsh, 2005), the base coordinates with the OH proton intact, as in Podjed *et al.* (2022).

A search for Cu coordinated by two ethanolamine ligands, with or without the OH proton, produced only three examples, *i.e.* Tudor *et al.* (2006), Vasileva *et al.* (1994), and the work by Jin *et al.* (2006) cited earlier.

Acknowledgements

We gratefully acknowledge support from the Chemistry Department at Fordham University and acknowledge assistance from Fordham student Nurul Eisha.

References

Blessing, R. H. (1989). *J. Appl. Cryst.* **22**, 396–397.
Burnett, M. N. & Johnson, C. K. (1996). *ORTEPIII*. Report ORNL6895. Oak Ridge National Laboratory, Tennessee, USA.
Corfield, P., Carlson, A., DaCunha, T., Eisha, N., Varona, A. M. F. & Garcia, D. (2022). *Acta Cryst.* A**78**, a192.
Corfield, P. W. R., Cleary, E. & Michalski, J. F. (2016). *Acta Cryst.* E**72**, 892–896.

Etaiw, S. E. H., Badr El-din, A. S. & Abdou, S. N. (2016). *Transition Met. Chem.* **41**, 413–425.
Farrugia, L. J. (2012). *J. Appl. Cryst.* **45**, 849–854.
Groom, C. R., Bruno, I. J., Lightfoot, M. P. & Ward, S. C. (2016). *Acta Cryst.* B**72**, 171–179.
Hathaway, B. J. (1971). *Essays in Chemistry*, Vol. 2, edited by J. N. Bradley, R. D. Gillard & R. F. Hudson, pp. 61–92. London: Academic Press.
Jin, Y., Che, Y. & Zheng, J. (2006). *J. Coord. Chem.* **59**, 691–698.
Kim, D. H., Koo, J. E., Hong, C. S., Oh, S. & Do, Y. (2005). *Inorg. Chem.* **44**, 4383–4390.
Koenigsmann, C., Rachid, L. N., Sheedy, C. M. & Corfield, P. W. R. (2020). *Acta Cryst.* C**76**, 405–411.
Lim, M. J., Murray, C. A., Tronic, T. A., deKrafft, K. E., Ley, A. N., deButts, J. C., Pike, R. D., Lu, H. & Patterson, H. H. (2008). *Inorg. Chem.* **47**, 6931–6947.
Liu, D. S., Chen, W. T., Ye, G.-M., Zhang, J. & Sui, Y. (2017). *J. Solid State Chem.* **256**, 14–18.
Marsh, R. E. (2005). *Acta Cryst.* B**61**, 359.
Nicholas, A. D., Bullard, R. M., Wheaton, A. M., Streep, M., Nicholas, V. A., Pike, R. D. & Patte, H. H. (2019). *Materials*, **12**, 1211.
Nieuwpoort, G., Verschoor, G. C. & Reedijk, J. (1983). *J. Chem. Soc. Dalton Trans.* pp. 531–538.
Nonius (1997). *KappaCCD Server Software*. Nonius BV, Delft, The Netherlands.
Otwinowski, Z. & Minor, W. (1997). *Methods in Enzymology*, Vol. 276, *Macromolecular Crystallography*, Part A, edited by C. W. Carter Jr & R. M. Sweet, pp. 307–326. New York: Academic Press.
Parkin, S., Moezzi, B. & Hope, H. (1995). *J. Appl. Cryst.* **28**, 53–56.
Pike, R. D. (2012). *Organometallics*, **31**, 7647–7660.
Podjed, N., Modec, B., Clérac, R., Rouzières, M., Alcaide, M. M. & López-Serrano, J. (2022). *New J. Chem.* **46**, 6899–6920.
Qin, Y., Wu, Y.-Q., Hou, J. J. & Zhang, X.-M. (2016). *Inorg. Chem. Commun.* **63**, 101–106.
Sheldrick, G. M. (2008). *Acta Cryst.* A**64**, 112–122.
Sheldrick, G. M. (2015*a*). *Acta Cryst.* A**71**, 3–8.
Sheldrick, G. M. (2015*b*). *Acta Cryst.* C**71**, 3–8.
Trivedi, M., Singh, G., Kumar, A. & Rath, N. P. (2014). *RSC Adv.* **4**, 34110–34116.
Tudor, V., Marin, G., Kavtsov, V., Simonov, Y. A., Julve, M., Lloet, F. & Andruh, M. (2006). *Rev. Roum. Chim.* **51**, 367–371.
Vasileva, O. Y., Kokozeii, V. N. & Skopenko, V. V. (1994). *Ukr. Khim. Zh.* **60**, 227.
Westrip, S. P. (2010). *J. Appl. Cryst.* **43**, 920–925.
Xu, H., Zhou, B.-Y., Yu, K., Su, Z.-H., Zhou, B.-B. & Su, Z.-M. (2019). *CrystEngComm*, **21**, 1242–1249.

supporting information

Acta Cryst. (2024). C**80**, 212-220 [https://doi.org/10.1107/S2053229624003371]

Crystal structures, electron spin resonance, and thermogravimetric analysis of three mixed-valence copper cyanide polymers

Peter W. R. Corfield, Ahmed Elsayed, Tristan DaCunha and Christopher Bender

Computing details

Poly[bis(*μ*-3-aminopropanolato)tetra-*μ*-cyanido-dicopper(I)dicopper(II)] (1)

Crystal data

$[Cu_4(CN)_4(C_3H_8NO)_2]$
M_r = 506.48
Monoclinic, *C*2/*c*
a = 9.6829 (4) Å
b = 8.2557 (4) Å
c = 21.4992 (10) Å
β = 95.212 (3)°
V = 1711.52 (14) Å^3
Z = 4
F(000) = 1000
D_x = 1.965 Mg m^{-3}
Mo *Kα* radiation, *λ* = 0.7107 Å
Cell parameters from 2094 reflections
θ = 27.5–1.0°
μ = 4.91 mm^{-1}
T = 295 K
Plate
0.31 × 0.15 × 0.08 mm

Data collection

Nonius KappaCCD diffractometer
Radiation source: fine-focus sealed tube
Graphite monochromator
Detector resolution: 9 pixels mm^{-1}
combination of *ω* and *φ* scans
Absorption correction: part of the refinement model (Δ*F*) (Otwinowski & Minor,1997)
T_{min} = 0.364, T_{max} = 0.514
19341 measured reflections
1965 independent reflections
1501 reflections with $I > 2\sigma(I)$
R_{int} = 0.048
θ_{max} = 27.5°, θ_{min} = 1.9°
h = 0→12
k = 0→10
l = −27→27

Refinement

Refinement on F^2
Least-squares matrix: full
$R[F^2 > 2\sigma(F^2)]$ = 0.025
$wR(F^2)$ = 0.074
S = 1.09
1965 reflections
124 parameters
0 restraints
Primary atom site location: structure-invariant direct methods
Secondary atom site location: structure-invariant direct methods
Hydrogen site location: mixed
H atoms treated by a mixture of independent and constrained refinement
$w = 1/[\sigma^2(F_o^2) + (0.041P)^2 + 0.370P]$ where $P = (F_o^2 + 2F_c^2)/3$
$(\Delta/\sigma)_{max}$ = 0.020
$\Delta\rho_{max}$ = 0.46 e Å^{-3}
$\Delta\rho_{min}$ = −0.42 e Å^{-3}

Special details

Geometry. All esds (except the esd in the dihedral angle between two l.s. planes) are estimated using the full covariance matrix. The cell esds are taken into account individually in the estimation of esds in distances, angles and torsion angles; correlations between esds in cell parameters are only used when they are defined by crystal symmetry. An approximate (isotropic) treatment of cell esds is used for estimating esds involving l.s. planes.

Fractional atomic coordinates and isotropic or equivalent isotropic displacement parameters (Å²)

	x	*y*	*z*	U_{iso}*/U_{eq}	Occ. (<1)
Cu1	0.64077 (3)	0.16386 (4)	0.29070 (2)	0.04609 (13)	
Cu2	0.27238 (3)	0.20602 (4)	0.43411 (2)	0.04478 (13)	
C1	0.5120 (3)	0.1789 (3)	0.35164 (13)	0.0487 (6)	
N1	0.4319 (2)	0.1869 (3)	0.38758 (11)	0.0549 (6)	
C2	0.7821 (2)	0.4657 (3)	0.23949 (11)	0.0482 (5)	0.5
N2	0.7298 (2)	0.3539 (3)	0.25912 (12)	0.0463 (5)	0.5
NC2	0.7821 (2)	0.4657 (3)	0.23949 (11)	0.0482 (5)	0.5
CN2	0.7298 (2)	0.3539 (3)	0.25912 (12)	0.0463 (5)	0.5
O11	0.12834 (17)	0.2377 (3)	0.48735 (8)	0.0542 (5)	
C12A	−0.0129 (16)	0.256 (2)	0.4727 (7)	0.062 (2)	0.743 (16)
H12A	−0.033862	0.368849	0.463114	0.074*	0.743 (16)
H12B	−0.062111	0.225074	0.508155	0.074*	0.743 (16)
C13A	−0.0623 (7)	0.1465 (11)	0.4143 (3)	0.0593 (17)	0.743 (16)
H13A	−0.040420	0.034439	0.424504	0.071*	0.743 (16)
H13B	−0.162217	0.155092	0.406362	0.071*	0.743 (16)
C14A	0.0032 (6)	0.1907 (11)	0.3548 (3)	0.0529 (14)	0.743 (16)
H14A	−0.004587	0.306501	0.347761	0.063*	0.743 (16)
H14B	−0.045675	0.135899	0.319475	0.063*	0.743 (16)
C12B	−0.025 (5)	0.234 (6)	0.464 (2)	0.062 (2)	0.257 (16)
H12C	−0.063636	0.137926	0.481483	0.074*	0.257 (16)
H12D	−0.067645	0.326126	0.482029	0.074*	0.257 (16)
C13B	−0.067 (2)	0.234 (4)	0.4077 (9)	0.066 (5)	0.257 (16)
H13C	−0.058832	0.343607	0.392293	0.079*	0.257 (16)
H13D	−0.165077	0.207764	0.404492	0.079*	0.257 (16)
C14B	−0.003 (2)	0.129 (3)	0.3666 (9)	0.0529 (14)	0.257 (16)
H14C	−0.050693	0.142574	0.325337	0.063*	0.257 (16)
H14D	−0.019577	0.018880	0.379565	0.063*	0.257 (16)
N15	0.1478 (3)	0.1439 (5)	0.36007 (13)	0.0648 (8)	
H15A	0.187 (5)	0.183 (6)	0.334 (2)	0.13 (2)*	
H15B	0.156 (4)	0.036 (6)	0.358 (2)	0.123 (18)*	

Atomic displacement parameters (Å²)

	U^{11}	U^{22}	U^{33}	U^{12}	U^{13}	U^{23}
Cu1	0.0428 (2)	0.0498 (2)	0.0478 (2)	−0.00036 (13)	0.01545 (14)	−0.00198 (14)
Cu2	0.03929 (19)	0.0620 (2)	0.03434 (19)	−0.00205 (13)	0.01053 (13)	−0.00526 (14)
C1	0.0483 (15)	0.0485 (16)	0.0508 (16)	−0.0018 (11)	0.0133 (13)	−0.0066 (12)
N1	0.0472 (12)	0.0756 (17)	0.0439 (13)	−0.0008 (11)	0.0156 (10)	−0.0081 (11)
C2	0.0504 (12)	0.0466 (14)	0.0491 (13)	0.0002 (11)	0.0125 (10)	−0.0030 (12)

N2	0.0484 (13)	0.0426 (13)	0.0495 (14)	−0.0010 (11)	0.0141 (11)	−0.0026 (11)
NC2	0.0504 (12)	0.0466 (14)	0.0491 (13)	0.0002 (11)	0.0125 (10)	−0.0030 (12)
CN2	0.0484 (13)	0.0426 (13)	0.0495 (14)	−0.0010 (11)	0.0141 (11)	−0.0026 (11)
O11	0.0337 (9)	0.0941 (14)	0.0356 (10)	−0.0013 (9)	0.0082 (7)	−0.0105 (10)
C12A	0.038 (4)	0.097 (5)	0.048 (5)	0.000 (3)	−0.002 (3)	−0.018 (4)
C13A	0.041 (2)	0.078 (4)	0.057 (3)	−0.008 (3)	0.000 (2)	−0.003 (3)
C14A	0.0490 (17)	0.067 (4)	0.041 (3)	−0.004 (3)	−0.0046 (18)	0.007 (3)
C12B	0.038 (4)	0.097 (5)	0.048 (5)	0.000 (3)	−0.002 (3)	−0.018 (4)
C13B	0.054 (8)	0.095 (15)	0.046 (8)	0.020 (11)	−0.007 (6)	−0.002 (10)
C14B	0.0490 (17)	0.067 (4)	0.041 (3)	−0.004 (3)	−0.0046 (18)	0.007 (3)
N15	0.0593 (16)	0.096 (2)	0.0393 (14)	−0.0091 (15)	0.0055 (12)	−0.0123 (15)

Geometric parameters (Å, º)

Cu1—C1	1.893 (3)	C13A—H13A	0.9700
Cu1—C2^{i}	1.935 (3)	C13A—H13B	0.9700
Cu1—N2	1.943 (2)	C14A—N15	1.447 (7)
Cu1—Cu1^{ii}	3.1030 (6)	C14A—H14A	0.9700
Cu2—O11	1.9011 (17)	C14A—H14B	0.9700
Cu2—O11^{iii}	1.9225 (18)	C12B—C13B	1.23 (5)
Cu2—N1	1.922 (2)	C12B—H12C	0.9700
Cu2—N15	1.976 (3)	C12B—H12D	0.9700
C1—N1	1.145 (4)	C13B—C14B	1.42 (3)
C2—N2	1.151 (3)	C13B—H13C	0.9700
O11—C12A	1.384 (16)	C13B—H13D	0.9700
O11—C12B	1.53 (5)	C14B—N15	1.48 (2)
C12A—C13A	1.586 (14)	C14B—H14C	0.9700
C12A—H12A	0.9700	C14B—H14D	0.9700
C12A—H12B	0.9700	N15—H15A	0.78 (5)
C13A—C14A	1.521 (12)	N15—H15B	0.90 (5)
C1—Cu1—C2^{i}	125.89 (10)	C13A—C14A—H14A	109.6
C1—Cu1—N2	122.02 (10)	N15—C14A—H14A	109.6
C2^{i}—Cu1—N2	111.63 (10)	C13A—C14A—H14B	109.6
C1—Cu1—Cu1^{ii}	77.89 (9)	N15—C14A—H14B	109.6
C2^{i}—Cu1—Cu1^{ii}	99.02 (7)	H14A—C14A—H14B	108.1
N2—Cu1—Cu1^{ii}	101.42 (8)	C13B—C12B—O11	124 (4)
O11—Cu2—O11^{iii}	76.91 (8)	C13B—C12B—H12C	106.4
O11—Cu2—N1	173.31 (9)	O11—C12B—H12C	106.5
O11^{iii}—Cu2—N1	96.64 (9)	C13B—C12B—H12D	106.4
O11—Cu2—N15	95.35 (10)	O11—C12B—H12D	106.5
O11^{iii}—Cu2—N15	172.04 (11)	H12C—C12B—H12D	106.5
N1—Cu2—N15	91.15 (11)	C12B—C13B—C14B	119 (3)
N1—C1—Cu1	178.5 (3)	C12B—C13B—H13C	107.6
C1—N1—Cu2	169.0 (2)	C14B—C13B—H13C	107.6
N2—C2—Cu1^{iv}	175.5 (2)	C12B—C13B—H13D	107.7
C2—N2—Cu1	178.9 (2)	C14B—C13B—H13D	107.6
C12A—O11—Cu2	129.9 (6)	H13C—C13B—H13D	107.1

C12B—O11—Cu2	122.6 (18)	C13B—C14B—N15	120 (2)
C12A—O11—Cu2^{iii}	125.4 (6)	C13B—C14B—H14C	107.3
Cu2—O11—Cu2^{iii}	103.09 (8)	N15—C14B—H14C	107.3
O11—C12A—C13A	109.8 (11)	C13B—C14B—H14D	107.3
O11—C12A—H12A	109.7	N15—C14B—H14D	107.3
C13A—C12A—H12A	109.7	H14C—C14B—H14D	106.9
O11—C12A—H12B	109.7	C14B—N15—Cu2	118.6 (8)
C13A—C12A—H12B	109.7	C14A—N15—Cu2	120.6 (3)
H12A—C12A—H12B	108.2	C14B—N15—H15A	131 (4)
C14A—C13A—C12A	114.2 (9)	C14A—N15—H15A	112 (4)
C14A—C13A—H13A	108.7	Cu2—N15—H15A	100 (4)
C12A—C13A—H13A	108.7	C14B—N15—H15B	91 (3)
C14A—C13A—H13B	108.7	C14A—N15—H15B	111 (3)
C12A—C13A—H13B	108.7	Cu2—N15—H15B	104 (3)
H13A—C13A—H13B	107.6	H15A—N15—H15B	109 (4)
C13A—C14A—N15	110.2 (7)		

Cu2—O11—C12A—C13A	35.5 (16)	Cu2^{iii}—O11—C12B—C13B	161 (3)
Cu2^{iii}—O11—C12A—C13A	−161.6 (6)	O11—C12B—C13B—C14B	46 (6)
O11—C12A—C13A—C14A	−62.3 (15)	C12B—C13B—C14B—N15	−59 (5)
C12A—C13A—C14A—N15	71.6 (13)	C13B—C14B—N15—Cu2	34 (3)
Cu2—O11—C12B—C13B	−11 (6)	C13A—C14A—N15—Cu2	−50.0 (9)

Symmetry codes: (i) −*x*+3/2, *y*−1/2, −*z*+1/2; (ii) −*x*+1, *y*, −*z*+1/2; (iii) −*x*+1/2, −*y*+1/2, −*z*+1; (iv) −*x*+3/2, *y*+1/2, −*z*+1/2.

Poly[bis(2-aminopropanol)tetra-μ-cyanido-tricopper(I,II)] (2)

Crystal data

$[Cu_3(CN)_4(C_3H_9NO)_2]$	$F(000)$ = 446
M_r = 444.94	D_x = 1.935 Mg m^{-3}
Monoclinic, $P2_1/c$	Mo $K\alpha$ radiation, λ = 0.7107 Å
a = 9.3903 (4) Å	Cell parameters from 1863 reflections
b = 8.9608 (4) Å	θ = 1.0–25.0°
c = 9.7986 (4) Å	μ = 4.15 mm^{-1}
β = 112.134 (3)°	T = 295 K
V = 763.74 (6) Å^3	Plate
Z = 2	0.15 × 0.08 × 0.02 mm

Data collection

Enraf-Nonius KappaCCD diffractometer	T_{min} = 0.75, T_{max} = 0.93
Radiation source: fine-focus sealed tube	19192 measured reflections
Graphite monochromator	1350 independent reflections
Detector resolution: 9 pixels mm^{-1}	855 reflections with $I > 2\sigma(I)$
combination of ω and φ scans	R_{int} = 0.084
Absorption correction: part of the refinement model (ΔF) (Otwinowski & Minor,1997)	θ_{max} = 25.0°, θ_{min} = 2.3°
	h = −11→10
	k = 0→10
	l = 0→11

Refinement

Refinement on F^2
Least-squares matrix: full
$R[F^2 > 2\sigma(F^2)] = 0.034$
$wR(F^2) = 0.113$
$S = 1.16$
1350 reflections
117 parameters
28 restraints
Primary atom site location: heavy-atom method
Secondary atom site location: difference Fourier map
Hydrogen site location: mixed
H atoms treated by a mixture of independent and constrained refinement
$w = 1/[\sigma^2(F_o^2) + (0.048P)^2 + 1.2P]$ where $P = (F_o^2 + 2F_c^2)/3$
$(\Delta/\sigma)_{max} < 0.001$
$\Delta\rho_{max} = 0.84$ e Å^{-3}
$\Delta\rho_{min} = -0.48$ e Å^{-3}

Special details

Geometry. All esds (except the esd in the dihedral angle between two l.s. planes) are estimated using the full covariance matrix. The cell esds are taken into account individually in the estimation of esds in distances, angles and torsion angles; correlations between esds in cell parameters are only used when they are defined by crystal symmetry. An approximate (isotropic) treatment of cell esds is used for estimating esds involving l.s. planes.

Fractional atomic coordinates and isotropic or equivalent isotropic displacement parameters (Å^2)

	x	*y*	*z*	U_{iso}*/U_{eq}	Occ. (<1)
Cu1	0.45669 (8)	−0.02366 (8)	−0.14833 (8)	0.0433 (3)	
Cu2	0.000000	0.000000	0.000000	0.0405 (3)	
C1	0.2964 (7)	−0.0113 (5)	−0.0678 (6)	0.0394 (13)	
N1	0.1857 (6)	−0.0090 (5)	−0.0474 (5)	0.0416 (11)	
C2	0.4991 (6)	0.2789 (6)	−0.2877 (6)	0.0482 (14)	0.5
N2	0.4823 (6)	0.1628 (6)	−0.2454 (6)	0.0425 (13)	0.5
C2N	0.4991 (6)	0.2789 (6)	−0.2877 (6)	0.0482 (14)	0.5
N2C	0.4823 (6)	0.1628 (6)	−0.2454 (6)	0.0425 (13)	0.5
O11A	0.121 (10)	0.212 (11)	0.196 (7)	0.055 (9)	0.537 (8)
H11A	0.190 (14)	0.272 (13)	0.207 (16)	0.065*	0.537 (8)
C12A	0.222 (2)	0.126 (2)	0.325 (2)	0.053 (3)	0.463 (8)
H12A	0.315574	0.094938	0.312100	0.080*	0.463 (8)
H12B	0.248953	0.182727	0.415081	0.080*	0.463 (8)
C13A	0.1207 (13)	−0.0068 (11)	0.3227 (11)	0.0373 (19)	0.537 (8)
H13A	0.017617	0.026093	0.312321	0.056*	0.537 (8)
N14A	0.1135 (5)	−0.1060 (5)	0.1972 (5)	0.0448 (12)	0.537 (8)
H14A	0.064638	−0.190114	0.200746	0.067*	0.537 (8)
H14B	0.208310	−0.129292	0.204899	0.067*	0.537 (8)
C15A	0.199 (3)	−0.092 (4)	0.467 (4)	0.075 (7)	0.537 (8)
H15A	0.204104	−0.029338	0.548490	0.113*	0.537 (8)
H15B	0.140548	−0.180008	0.466991	0.113*	0.537 (8)
H15C	0.300891	−0.119842	0.476832	0.113*	0.537 (8)
O11B	0.132 (12)	0.213 (13)	0.175 (8)	0.055 (9)	0.463 (8)
H11B	0.211 (14)	0.232 (17)	0.162 (16)	0.065*	0.463 (8)
C12B	0.1572 (18)	0.137 (2)	0.316 (2)	0.053 (3)	0.537 (8)
H12C	0.060844	0.130492	0.330578	0.080*	0.537 (8)
H12D	0.228706	0.194823	0.396615	0.080*	0.537 (8)
C13B	0.2200 (15)	−0.0148 (12)	0.3157 (13)	0.0373 (19)	0.463 (8)

H13B	0.312585	−0.002539	0.293205	0.056*	0.463 (8)
N14B	0.1135 (5)	−0.1060 (5)	0.1972 (5)	0.0448 (12)	0.463 (8)
H14C	0.043546	−0.143775	0.228563	0.067*	0.463 (8)
H14D	0.165766	−0.182183	0.180980	0.067*	0.463 (8)
C15B	0.271 (3)	−0.088 (4)	0.464 (5)	0.075 (7)	0.463 (8)
H15D	0.310254	−0.185476	0.458921	0.113*	0.463 (8)
H15E	0.349447	−0.028548	0.534644	0.113*	0.463 (8)
H15F	0.184552	−0.096094	0.493930	0.113*	0.463 (8)

Atomic displacement parameters (Å²)

	U^{11}	U^{22}	U^{33}	U^{12}	U^{13}	U^{23}
Cu1	0.0462 (5)	0.0420 (4)	0.0483 (5)	−0.0008 (3)	0.0252 (4)	−0.0008 (3)
Cu2	0.0340 (6)	0.0501 (6)	0.0400 (6)	0.0018 (4)	0.0168 (4)	0.0005 (4)
C1	0.041 (3)	0.033 (3)	0.053 (4)	0.001 (2)	0.027 (3)	0.005 (2)
N1	0.036 (3)	0.049 (3)	0.042 (3)	0.002 (2)	0.018 (2)	0.002 (2)
C2	0.044 (3)	0.051 (4)	0.050 (4)	0.000 (3)	0.019 (3)	0.001 (3)
N2	0.046 (3)	0.035 (3)	0.047 (3)	−0.004 (2)	0.019 (3)	0.004 (2)
C2N	0.044 (3)	0.051 (4)	0.050 (4)	0.000 (3)	0.019 (3)	0.001 (3)
N2C	0.046 (3)	0.035 (3)	0.047 (3)	−0.004 (2)	0.019 (3)	0.004 (2)
O11A	0.066 (10)	0.045 (3)	0.059 (14)	−0.008 (6)	0.031 (10)	0.004 (11)
C12A	0.058 (8)	0.045 (4)	0.056 (4)	0.002 (6)	0.019 (6)	0.001 (3)
C13A	0.042 (4)	0.040 (4)	0.036 (3)	0.001 (4)	0.022 (4)	−0.004 (3)
N14A	0.047 (3)	0.044 (3)	0.043 (3)	−0.001 (2)	0.016 (2)	−0.002 (2)
C15A	0.10 (2)	0.056 (5)	0.048 (5)	−0.001 (13)	0.003 (15)	0.003 (4)
O11B	0.066 (10)	0.045 (3)	0.059 (14)	−0.008 (6)	0.031 (10)	0.004 (11)
C12B	0.058 (8)	0.045 (4)	0.056 (4)	0.002 (6)	0.019 (6)	0.001 (3)
C13B	0.042 (4)	0.040 (4)	0.036 (3)	0.001 (4)	0.022 (4)	−0.004 (3)
N14B	0.047 (3)	0.044 (3)	0.043 (3)	−0.001 (2)	0.016 (2)	−0.002 (2)
C15B	0.10 (2)	0.056 (5)	0.048 (5)	−0.001 (13)	0.003 (15)	0.003 (4)

Geometric parameters (Å, º)

Cu1—C1	1.948 (6)	C13A—H13A	0.9800
Cu1—C2^{i}	1.973 (5)	N14A—H14A	0.8900
Cu1—N2	1.982 (5)	N14A—H14B	0.8900
Cu1—C1^{ii}	2.502 (6)	C15A—H15A	0.9600
Cu1—Cu1^{ii}	2.7403 (14)	C15A—H15B	0.9600
Cu2—N1	1.969 (5)	C15A—H15C	0.9600
Cu2—N14B	2.054 (5)	O11B—C12B	1.47 (3)
Cu2—N14A	2.054 (5)	O11B—H11B	0.82 (2)
Cu2—O11A	2.64 (11)	C12B—C13B	1.49 (2)
Cu2—O11B	2.56 (13)	C12B—H12C	0.9700
C1—N1	1.130 (8)	C12B—H12D	0.9700
C2—N2	1.152 (7)	C13B—C15B	1.50 (4)
O11A—C12A	1.47 (3)	C13B—N14B	1.463 (13)
O11A—H11A	0.82 (2)	C13B—H13B	0.9800
C12A—C13A	1.52 (2)	N14B—H14C	0.8900

C12A—H12A	0.9700	N14B—H14D	0.8900
C12A—H12B	0.9700	C15B—H15D	0.9600
C13A—N14A	1.497 (10)	C15B—H15E	0.9600
C13A—C15A	1.53 (4)	C15B—H15F	0.9600

C1—Cu1—C2^{i}	117.8 (2)	N14A—C13A—H13A	110.9
C1—Cu1—N2	113.5 (2)	C12A—C13A—H13A	110.9
C2^{i}—Cu1—N2	121.7 (2)	C15A—C13A—H13A	110.9
C1—Cu1—C1^{ii}	105.1 (2)	C13A—N14A—Cu2	110.2 (5)
C2^{i}—Cu1—C1^{ii}	98.19 (19)	C13A—N14A—H14A	109.6
N2—Cu1—C1^{ii}	93.39 (19)	Cu2—N14A—H14A	109.6
C1—Cu1—Cu1^{ii}	61.80 (18)	C13A—N14A—H14B	109.6
C2^{i}—Cu1—Cu1^{ii}	117.51 (16)	Cu2—N14A—H14B	109.6
N2—Cu1—Cu1^{ii}	109.72 (16)	H14A—N14A—H14B	108.1
C1^{ii}—Cu1—Cu1^{ii}	43.34 (13)	C13A—C15A—H15A	109.5
N1^{iii}—Cu2—N1	180.0 (2)	C13A—C15A—H15B	109.5
N1^{iii}—Cu2—N14A^{iii}	90.66 (18)	H15A—C15A—H15B	109.5
N1—Cu2—N14A^{iii}	89.34 (18)	C13A—C15A—H15C	109.5
N1^{iii}—Cu2—N14B	89.34 (18)	H15A—C15A—H15C	109.5
N1—Cu2—N14B	90.66 (18)	H15B—C15A—H15C	109.5
N1^{iii}—Cu2—N14A	89.34 (18)	C12B—O11B—Cu2	99 (6)
N1—Cu2—N14A	90.66 (18)	C12B—O11B—H11B	114 (10)
N14A^{iii}—Cu2—N14A	180.0	Cu2—O11B—H11B	106 (10)
N1^{iii}—Cu2—O11A	89 (2)	O11B—C12B—C13B	110 (5)
N1—Cu2—O11A	91 (2)	O11B—C12B—H12C	109.6
N14A^{iii}—Cu2—O11A	106.4 (8)	C13B—C12B—H12C	109.6
N14A—Cu2—O11A	73.6 (8)	O11B—C12B—H12D	109.6
N1^{iii}—Cu2—O11B	93 (3)	C13B—C12B—H12D	109.6
N1—Cu2—O11B	87 (3)	H12C—C12B—H12D	108.1
N14B—Cu2—O11B	76.5 (8)	C15B—C13B—C12B	112.3 (18)
N1—C1—Cu1	167.2 (6)	C15B—C13B—N14B	113.5 (16)
N1—C1—Cu1^{ii}	118.0 (5)	C12B—C13B—N14B	111.1 (10)
Cu1—C1—Cu1^{ii}	74.9 (2)	C15B—C13B—H13B	106.5
C1—N1—Cu2	176.5 (5)	C12B—C13B—H13B	106.5
N2—C2—Cu1^{iv}	176.0 (5)	N14B—C13B—H13B	106.5
C2—N2—Cu1	172.6 (5)	C13B—N14B—Cu2	116.5 (5)
C12A—O11A—Cu2	102 (5)	C13B—N14B—H14C	108.2
C12A—O11A—H11A	91 (10)	Cu2—N14B—H14C	108.2
Cu2—O11A—H11A	132 (10)	C13B—N14B—H14D	108.2
C13A—C12A—O11A	101 (4)	Cu2—N14B—H14D	108.2
C13A—C12A—H12A	111.5	H14C—N14B—H14D	107.3
O11A—C12A—H12A	111.5	C13B—C15B—H15D	109.5
C13A—C12A—H12B	111.5	C13B—C15B—H15E	109.5
O11A—C12A—H12B	111.5	H15D—C15B—H15E	109.5
H12A—C12A—H12B	109.3	C13B—C15B—H15F	109.5
N14A—C13A—C12A	108.0 (10)	H15D—C15B—H15F	109.5
N14A—C13A—C15A	108.8 (14)	H15E—C15B—H15F	109.5
C12A—C13A—C15A	107.4 (14)		

Cu2—O11A—C12A—C13A	−42 (4)	Cu2—O11B—C12B—C13B	46 (5)
O11A—C12A—C13A—N14A	73 (4)	O11B—C12B—C13B—C15B	171 (5)
O11A—C12A—C13A—C15A	−169 (5)	O11B—C12B—C13B—N14B	−61 (5)
C12A—C13A—N14A—Cu2	−66.5 (10)	C15B—C13B—N14B—Cu2	166.7 (14)
C15A—C13A—N14A—Cu2	177.3 (10)	C12B—C13B—N14B—Cu2	39.0 (12)

Symmetry codes: (i) −*x*+1, *y*−1/2, −*z*−1/2; (ii) −*x*+1, −*y*, −*z*; (iii) −*x*, −*y*, −*z*; (iv) −*x*+1, *y*+1/2, −*z*−1/2.

Hydrogen-bond geometry (Å, º)

D—H···*A*	*D*—H	H···*A*	*D*···*A*	*D*—H···*A*
N14*A*—H14*A*···O11*A*^{v}	0.89	2.48	3.21 (11)	140
O11*B*—H11*B*···N2^{vi}	0.82 (2)	2.54 (13)	3.28 (11)	150 (13)
C12*A*—H12*A*···C2N^{vi}	0.97	2.54	3.29 (2)	134

Symmetry codes: (v) −*x*, *y*−1/2, −*z*+1/2; (vi) *x*, −*y*+1/2, *z*+1/2.

Poly[bis(2-aminoethanol)tetra-*μ*-cyanido-tricopper(II)] (3)

Crystal data

$[Cu_3(CN)_4(C_2H_7NO)_2]$
M_r = 416.88
Monoclinic, $P2_1/c$
a = 9.5158 (2) Å
b = 8.8022 (2) Å
c = 9.3589 (2) Å
β = 117.358 (1)°
V = 696.22 (3) Å^3
Z = 2
F(000) = 414
D_x = 1.989 Mg m^{-3}
Mo *Kα* radiation, *λ* = 0.7107 Å
Cell parameters from 2164 reflections
θ = 1.0–28.8°
μ = 4.55 mm^{-1}
T = 295 K
Block
0.37 × 0.25 × 0.22 mm

Data collection

Enraf-Nonius KappaCCD diffractometer
Radiation source: fine-focus sealed tube
Graphite monochromator
Detector resolution: 9 pixels mm^{-1}
combination of *ω* and *φ* scans
Absorption correction: part of the refinement model (Δ*F*) (Otwinowski & Minor,1997)
T_{min} = 0.48, T_{max} = 0.59
27010 measured reflections
1740 independent reflections
1049 reflections with $I > 2\sigma(I)$
R_{int} = 0.046
θ_{max} = 28.8°, θ_{min} = 2.4°
h = −11→11
k = 0→11
l = 0→12

Refinement

Refinement on F^2
Least-squares matrix: full
$R[F^2 > 2\sigma(F^2)]$ = 0.024
$wR(F^2)$ = 0.077
S = 1.16
1740 reflections
118 parameters
26 restraints
Primary atom site location: heavy-atom method
Secondary atom site location: difference Fourier map
Hydrogen site location: mixed
H atoms treated by a mixture of independent and constrained refinement
$w = 1/[\sigma^2(F_o^2) + (0.0263P)^2 + 0.630P]$ where $P = (F_o^2 + 2F_c^2)/3$
$(\Delta/\sigma)_{max}$ = 0.006
$\Delta\rho_{max}$ = 1.07 e Å^{-3}
$\Delta\rho_{min}$ = −0.53 e Å^{-3}
Extinction correction: SHELXL2018 (Sheldrick, 2015*b*), $Fc^*=kFc[1+0.001xFc^2\lambda^3/\sin(2\theta)]^{-1/4}$
Extinction coefficient: 0.0030 (8)

Special details

Geometry. All esds (except the esd in the dihedral angle between two l.s. planes) are estimated using the full covariance matrix. The cell esds are taken into account individually in the estimation of esds in distances, angles and torsion angles; correlations between esds in cell parameters are only used when they are defined by crystal symmetry. An approximate (isotropic) treatment of cell esds is used for estimating esds involving l.s. planes.

Fractional atomic coordinates and isotropic or equivalent isotropic displacement parameters (Å²)

	x	*y*	*z*	U_{iso}*/U_{eq}	Occ. (<1)
Cu1	0.43137 (4)	−0.00194 (4)	−0.16664 (4)	0.03507 (14)	
Cu2	0.000000	0.000000	0.000000	0.02951 (14)	
C1	0.2785 (3)	0.0024 (3)	−0.0860 (3)	0.0351 (5)	
N1	0.1773 (3)	0.0056 (3)	−0.0525 (3)	0.0369 (5)	
C2	0.5179 (3)	0.3029 (3)	−0.2702 (3)	0.0378 (6)	0.5
N2	0.4816 (3)	0.1875 (3)	−0.2405 (3)	0.0398 (6)	0.5
N2C	0.5179 (3)	0.3029 (3)	−0.2702 (3)	0.0378 (6)	0.5
C2N	0.4816 (3)	0.1875 (3)	−0.2405 (3)	0.0398 (6)	0.5
O11A	0.1498 (19)	−0.1514 (11)	0.241 (2)	0.0534 (15)	0.643 (14)
H11A	0.202 (8)	−0.226 (5)	0.243 (10)	0.051 (15)*	0.643 (14)
C12A	0.2544 (10)	−0.0467 (8)	0.3618 (7)	0.0484 (19)	0.643 (14)
H12A	0.290950	−0.088854	0.468798	0.073*	0.643 (14)
H12B	0.345489	−0.023671	0.345150	0.073*	0.643 (14)
C13A	0.1569 (11)	0.0924 (7)	0.3410 (6)	0.0475 (19)	0.643 (14)
H13A	0.063915	0.066997	0.353403	0.071*	0.643 (14)
H13B	0.217945	0.167214	0.421944	0.071*	0.643 (14)
N14A	0.1096 (3)	0.1541 (3)	0.1812 (3)	0.0448 (6)	0.643 (14)
H14A	0.195028	0.189574	0.176700	0.067*	0.643 (14)
H14B	0.044412	0.232000	0.165357	0.067*	0.643 (14)
O11B	0.143 (4)	−0.189 (2)	0.249 (4)	0.0534 (15)	0.357 (14)
H11B	0.220 (11)	−0.197 (13)	0.232 (17)	0.051 (15)*	0.357 (14)
C12B	0.171 (2)	−0.0648 (17)	0.3598 (13)	0.058 (3)	0.357 (14)
H12C	0.241443	−0.100736	0.467296	0.087*	0.357 (14)
H12D	0.071231	−0.039347	0.358141	0.087*	0.357 (14)
C13B	0.2362 (19)	0.0704 (15)	0.3333 (12)	0.050 (3)	0.357 (14)
H13C	0.327766	0.046259	0.317901	0.075*	0.357 (14)
H13D	0.270322	0.136169	0.426513	0.075*	0.357 (14)
N14B	0.1096 (3)	0.1541 (3)	0.1812 (3)	0.0448 (6)	0.357 (14)
H14C	0.155966	0.225597	0.150299	0.067*	0.357 (14)
H14D	0.038556	0.198626	0.204402	0.067*	0.357 (14)

Atomic displacement parameters (Å²)

	U^{11}	U^{22}	U^{33}	U^{12}	U^{13}	U^{23}
Cu1	0.0384 (2)	0.0342 (2)	0.0408 (2)	0.00048 (17)	0.02519 (16)	0.00040 (16)
Cu2	0.0272 (2)	0.0342 (2)	0.0311 (2)	−0.0012 (2)	0.01687 (18)	−0.0013 (2)
C1	0.0394 (13)	0.0296 (13)	0.0433 (14)	−0.0010 (14)	0.0250 (12)	−0.0014 (13)
N1	0.0327 (11)	0.0432 (13)	0.0388 (12)	−0.0015 (12)	0.0197 (10)	−0.0033 (11)
C2	0.0401 (15)	0.0334 (14)	0.0416 (15)	0.0005 (11)	0.0203 (12)	0.0064 (11)

N2	0.0392 (15)	0.0414 (16)	0.0399 (14)	0.0027 (12)	0.0190 (12)	0.0056 (12)
N2C	0.0401 (15)	0.0334 (14)	0.0416 (15)	0.0005 (11)	0.0203 (12)	0.0064 (11)
C2N	0.0392 (15)	0.0414 (16)	0.0399 (14)	0.0027 (12)	0.0190 (12)	0.0056 (12)
O11A	0.061 (2)	0.022 (5)	0.081 (3)	0.013 (4)	0.0363 (17)	0.018 (5)
C12A	0.039 (3)	0.059 (3)	0.041 (3)	0.011 (3)	0.013 (2)	0.002 (2)
C13A	0.048 (4)	0.060 (3)	0.034 (2)	0.010 (3)	0.018 (2)	−0.004 (2)
N14A	0.0484 (14)	0.0414 (14)	0.0500 (15)	−0.0048 (12)	0.0274 (12)	−0.0040 (12)
O11B	0.061 (2)	0.022 (5)	0.081 (3)	0.013 (4)	0.0363 (17)	0.018 (5)
C12B	0.051 (5)	0.097 (6)	0.042 (4)	−0.021 (4)	0.035 (4)	−0.010 (4)
C13B	0.046 (5)	0.054 (5)	0.044 (4)	−0.007 (4)	0.015 (4)	−0.008 (4)
N14B	0.0484 (14)	0.0414 (14)	0.0500 (15)	−0.0048 (12)	0.0274 (12)	−0.0040 (12)

Geometric parameters (Å, º)

Cu1—C1	1.922 (3)	C13A—N14A	1.454 (6)
Cu1—N2	1.947 (3)	C13A—H13A	0.9700
Cu1—C2^{i}	1.949 (3)	C13A—H13B	0.9700
Cu1—Cu1^{ii}	2.7734 (7)	N14A—H14A	0.8900
Cu2—N1	1.963 (2)	N14A—H14B	0.8900
Cu2—N14A	2.044 (2)	O11B—C12B	1.44 (3)
Cu2—N14B	2.044 (2)	O11B—H11B	0.819 (10)
Cu2—O11B	2.67 (3)	C12B—C13B	1.41 (2)
Cu2—O11A	2.439 (14)	C12B—H12C	0.9700
C1—N1	1.142 (4)	C12B—H12D	0.9700
C2—N2	1.147 (4)	C13B—N14B	1.563 (12)
O11A—C12A	1.442 (17)	C13B—H13C	0.9700
O11A—H11A	0.817 (10)	C13B—H13D	0.9700
C12A—C13A	1.494 (11)	N14B—H14C	0.8900
C12A—H12A	0.9700	N14B—H14D	0.8900
C12A—H12B	0.9700		
C1—Cu1—N2	118.41 (12)	O11A—C12A—H12A	110.8
C1—Cu1—C2^{i}	118.33 (12)	C13A—C12A—H12B	110.8
N2—Cu1—C2^{i}	120.78 (11)	O11A—C12A—H12B	110.8
C1—Cu1—Cu1^{ii}	66.96 (9)	H12A—C12A—H12B	108.8
N2—Cu1—Cu1^{ii}	108.86 (8)	N14A—C13A—C12A	108.7 (6)
C2^{i}—Cu1—Cu1^{ii}	107.33 (8)	N14A—C13A—H13A	109.9
N1—Cu2—N1^{iii}	180.0	C12A—C13A—H13A	109.9
N1—Cu2—N14A^{iii}	88.76 (10)	N14A—C13A—H13B	109.9
N1^{iii}—Cu2—N14A^{iii}	91.24 (10)	C12A—C13A—H13B	109.9
N1—Cu2—N14A	91.24 (10)	H13A—C13A—H13B	108.3
N1^{iii}—Cu2—N14A	88.76 (10)	C13A—N14A—Cu2	113.8 (3)
N14A^{iii}—Cu2—N14A	180.0	C13A—N14A—H14A	108.8
N1—Cu2—N14B	91.24 (10)	Cu2—N14A—H14A	108.8
N1^{iii}—Cu2—N14B	88.76 (10)	C13A—N14A—H14B	108.8
N1—Cu2—O11B^{iii}	85.3 (7)	Cu2—N14A—H14B	108.8
N1^{iii}—Cu2—O11B^{iii}	94.7 (7)	H14A—N14A—H14B	107.7
N14A^{iii}—Cu2—O11B^{iii}	80.1 (7)	C12B—O11B—Cu2	90.3 (10)

N14A—Cu2—O11B^{iii}	99.9 (7)	C12B—O11B—H11B	109 (10)
N14B—Cu2—O11B^{iii}	99.9 (7)	Cu2—O11B—H11B	91 (9)
N1—Cu2—O11B	94.7 (7)	O11B—C12B—C13B	117.6 (14)
N1^{iii}—Cu2—O11B	85.3 (7)	O11B—C12B—H12C	107.9
N14B—Cu2—O11B	80.1 (7)	C13B—C12B—H12C	107.9
O11B^{iii}—Cu2—O11B	180.0	O11B—C12B—H12D	107.9
N1—Cu2—O11A	92.4 (4)	C13B—C12B—H12D	107.9
N1^{iii}—Cu2—O11A	87.6 (4)	H12C—C12B—H12D	107.2
N14A^{iii}—Cu2—O11A	105.3 (3)	C12B—C13B—N14B	109.9 (12)
N14A—Cu2—O11A	74.7 (3)	C12B—C13B—H13C	109.7
N1—C1—Cu1	173.7 (3)	N14B—C13B—H13C	109.7
N1—C1—Cu1^{ii}	114.4 (2)	C12B—C13B—H13D	109.7
Cu1—C1—Cu1^{ii}	71.84 (9)	N14B—C13B—H13D	109.7
C1—N1—Cu2	176.9 (2)	H13C—C13B—H13D	108.2
N2—C2—Cu1^{iv}	176.5 (3)	C13B—N14B—Cu2	109.2 (5)
C2—N2—Cu1	174.0 (3)	C13B—N14B—H14C	109.8
C12A—O11A—Cu2	106.0 (5)	Cu2—N14B—H14C	109.8
C12A—O11A—H11A	108 (6)	C13B—N14B—H14D	109.8
Cu2—O11A—H11A	123 (6)	Cu2—N14B—H14D	109.8
C13A—C12A—O11A	104.9 (8)	H14C—N14B—H14D	108.3
C13A—C12A—H12A	110.8		

Symmetry codes: (i) −*x*+1, *y*−1/2, −*z*−1/2; (ii) −*x*+1, −*y*, −*z*; (iii) −*x*, −*y*, −*z*; (iv) −*x*+1, *y*+1/2, −*z*−1/2.

Hydrogen-bond geometry (Å, º)

D—H···*A*	*D*—H	H···*A*	*D*···*A*	*D*—H···*A*
N14*B*—H14*D*···O11*B*^{v}	0.89	2.20	3.09 (3)	178
O11*B*—H11*B*···N2*C*^{ii}	0.82 (1)	2.53 (6)	3.30 (3)	156 (11)

Symmetry codes: (ii) −*x*+1, −*y*, −*z*; (v) −*x*, *y*+1/2, −*z*+1/2.